



RESEARCH ARTICLE

10.1002/2015RS005919

Key Points:

- A quality factor is defined for the MUF values provided by OIASA algorithm
- The oblique ionograms are converted into vertical and analyzed by Autoscala
- The quality factor is based on the f_oF_2 obtained by the autoscaling of the vertical ionograms

Correspondence to:

A. Ippolito,
alessandro.ippolito@ingv.it

Citation:

Ippolito, A., C. Scotto, D. Sabbagh, V. Sgrigna, and P. Maher (2016), A procedure for the reliability improvement of the oblique ionograms automatic scaling algorithm, *Radio Sci.*, 51, 454–460, doi:10.1002/2015RS005919.

Received 11 DEC 2015

Accepted 5 APR 2016

Accepted article online 8 APR 2016

Published online 17 MAY 2016

A procedure for the reliability improvement of the oblique ionograms automatic scaling algorithm

Alessandro Ippolito¹, Carlo Scotto¹, Dario Sabbagh^{1,2}, Vittorio Sgrigna², and Phillip Maher³

¹Istituto Nazionale di Geofisica e Vulcanologia, Rome, Italy, ²Dipartimento di Matematica e Fisica, Università degli Studi Roma Tre, Rome, Italy, ³Space Weather Services, Bureau of Meteorology, Sydney, New South Wales, Australia

Abstract A procedure made by the combined use of the Oblique Ionogram Automatic Scaling Algorithm (OIASA) and Autoscala program is presented. Using Martyn's equivalent path theorem, 384 oblique soundings from a high-quality data set have been converted into vertical ionograms and analyzed by Autoscala program. The ionograms pertain to the radio link between Curtin W.A. (CUR) and Alice Springs N.T. (MTE), Australia, geographical coordinates (17.60°S; 123.82°E) and (23.52°S; 133.68°E), respectively. The critical frequency f_oF_2 values extracted from the converted vertical ionograms by Autoscala were then compared with the f_oF_2 values derived from the maximum usable frequencies (MUFs) provided by OIASA. A quality factor Q for the MUF values autoscaled by OIASA has been identified. Q represents the difference between the f_oF_2 value scaled by Autoscala from the converted vertical ionogram and the f_oF_2 value obtained applying the secant law to the MUF provided by OIASA. Using the receiver operating characteristic curve, an appropriate threshold level Q_t was chosen for Q to improve the performance of OIASA.

1. Introduction

Currently, the knowledge of the real-time state of the ionosphere relies on the application of assimilative techniques into both physical and empirical models. For this purpose, real-time ionospheric data are required. Interestingly, the Earth's ionosphere was discovered by the observations of radio waves reflected by an unknown layer. Following Marconi's experiments, a number of pioneers of wireless [Kennelly, 1902; Heaviside, 1902; Lodge, 1902] stated that waves properties could only be explained by the presence of a reflecting layer composed of electrons and positive ions. The existence of such a layer was demonstrated in 1925 by Edward Appleton together with his student Miles Barnett [Bibl, 1998]. In subsequent years, the technique was refined to the point of recording a graph $t(f)$ of the time t elapsed for a radio frequency f to travel the ionosphere-Earth-ionosphere path onto a film, the device being called an ionosonde. Networks of ionosondes are now routinely used to measure the characteristics of the ionosphere. Well-established techniques, such as the Automatic Real Time Ionogram Scaler with True Height Analysis system [Reinisch and Huang, 1983; Gilbert and Smith, 1988; Galkin et al., 2008] and the Autoscala program [Scotto and Pezzopane, 2002a, 2002b; Pezzopane and Scotto, 2007; Scotto, 2009], make it possible to obtain the main ionospheric characteristics, such as the critical frequencies of the different ionospheric layers and the related virtual heights, in real time from vertical ionograms [Scotto and Pezzopane, 2008]. The output data provided by these software packages can be integrated in real time and provide short term forecasting models [Galkin et al., 2012]. Unlike vertical soundings, for which transmitter and receiver are collocated, for oblique ionospheric soundings the transmitter and the receiver are generally several hundreds or thousands of kilometers apart, such that the radio waves are obliquely incident on the ionosphere. The oblique ionogram that one obtains from this kind of measurement (Figure 1a) is a representation of the time delay versus the frequency response of the ionosphere, for the considered radio link. The interpretation of ionospheric parameters from oblique ionograms is significantly more complex when compared to the vertical ionograms, and there are no well-established automatic techniques. Oblique soundings are mainly used to understand the factors that attenuate and distort the propagation of radio wave in the high-frequency (HF) range through the ionized layer of the Earth's atmosphere, in order to improve radio link reliability caused by this natural variability of the ionosphere.

2. Automatic Scaling of Oblique Ionograms

In the absence of an automatic procedure for the interpretation of the oblique ionograms, time intensive manual methods are required in order to individually scale them. However, with the growing interest in

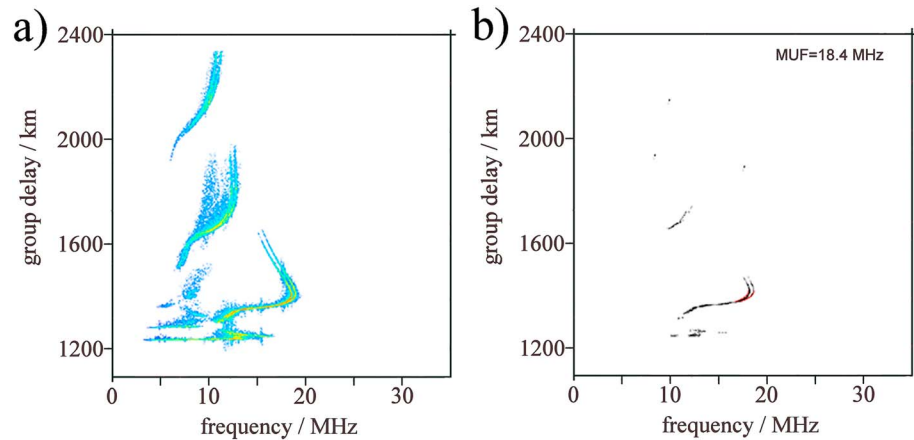


Figure 1. The results of the application of the noise filtering algorithm. An ionogram (a) before and (b) after the application of the noise filter.

the acquisition of real-time ionospheric data for correcting propagation delays in satellite communications, predicting space weather, and ionospheric disturbances due to geomagnetic storms and solar flares [Jin *et al.*, 2006; Cushley and Noel, 2014], this has highlighted the need for the automatic scaling of oblique ionograms [Redding, 1996]. In addition, oblique ionospheric sounding also offers several important advantages over vertical sounding. For example, the opportunity of monitoring the ionosphere across large, otherwise inaccessible areas such as ocean surfaces and the ability of a receiver to detect signals from many different directions. Despite the fact that oblique ionogram inversion methods have received less attention than the inversion of the vertical ionograms, several attempts have been made in order to derive the midpoint electron density profile from oblique soundings. Gething and Maliphant [1967] suggested a double-step method in which an oblique ionogram is converted into a vertical and analyzed by means of inversion techniques developed for vertical ionograms. A further approach is to obtain the electron density profile directly from the oblique ionogram, as has been proposed by Phanivong *et al.* [1995]. This method takes into account the presence of the Earth’s magnetic field and is based on the inversion technique developed by Reilly and Kolesar [1989], which considers the curvature of the ionosphere and handles the ambiguity related to the presence of the valley in the electron density profile. In the work presented here, we propose a quality factor for the MUF values provided by Oblique Ionogram Automatic Scaling Algorithm (OIASA) [Ippolito *et al.*, 2015]. Applying OIASA to an oblique ionogram, we obtain the autoscaled value of maximum usable frequency, $MUF_{[OIASA]}$, from which we derive the critical frequency of the F_2 layer through the secant law. The autoscaled oblique ionogram is then converted into a vertical one and then analyzed by the Autoscala program in order to obtain the critical frequency f_oF_2 . The two values of f_oF_2 , resulting from the two different procedures are then compared. The reliability of $MUF_{[OIASA]}$ is assessed in this way, and a technique to discard the cases of erroneous interpretation is consequently introduced.

3. Oblique to Vertical Ionograms Conversion

The procedure to convert an oblique ionogram into a vertical one begins with the storage of the oblique sounding in matrix form. The number of rows m and columns n of the matrix A are defined by the following formulas:

$$m = \text{int} \left[\frac{(t_f - t_0)}{\Delta t} \right], \tag{1}$$

and

$$n = \text{int} \left[\frac{(f_f - f_0)}{\Delta f} \right] \tag{2}$$

where *int* stands for integer; f_f , f_0 , Δf , t_f , t_0 , and Δt are, respectively, the final frequency, the initial frequency, the frequency step, the final time delay, the initial time delay, and the time delay resolution of the oblique sounding. The values t_0 and Δt are fixed and depend on the design of the ionosonde. The values f_0 , f_f and Δf , are usually set in accordance with the programmed measurement campaign. The element a_{ij}

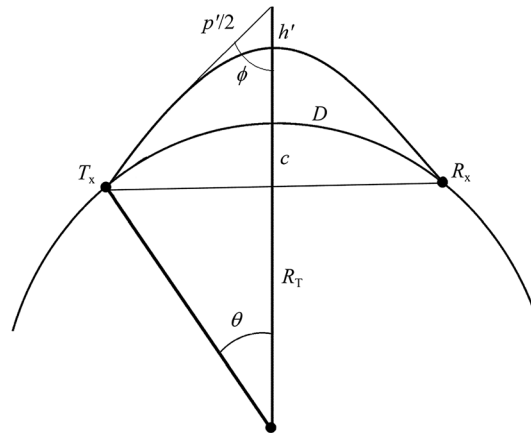


Figure 2. A scheme of the considered geometry for an oblique ray path, where T_x and R_x represent, respectively, the transmitter and the receiver. The Earth's curvature is also taken into account.

of pixels, chosen with the nearest neighbor technique around the considered element a_{ij} , are analyzed and their numerical values are summed up. When this sum is greater than a fixed threshold, the element a_{ij} is assumed to be part of the noise and then deleted. Once the ionograms background noise is filtered, every element a_{ij} of the matrix A represents a frequency-virtual ray path pair. Applying the secant law and the Martyn's equivalent path theorem [Martyn, 1935] to each element a_{ij} , the equivalent vertical ionogram is obtained. According to the geometry of the oblique ray path shown schematically in Figure 2, the curvature of the Earth is also considered. Taking into account an isotropic, horizontally homogeneous, and flat ionosphere and representing f_o and f_v as the frequencies of the radio waves reflected obliquely and vertically respectively, at the same real height, from the secant law we have

$$f_v = \frac{f_o}{\sec\phi}, \tag{3}$$

where ϕ is the incidence angle of the high-frequency radio signal. According to the Martyn's theorem, the virtual height at which f_v is reflected from the ionosphere is given by [Gething, 1969; Kol'tsov, 1969]:

$$h'(f_v) = \frac{p'(f_o)}{2\sec\phi} - c. \tag{4}$$

Through geometric considerations we also have

$$c = R_T(1 - \cos\theta), \tag{5}$$

and

$$\phi = \sin^{-1} \frac{D}{p'(f_o)}. \tag{6}$$

where h' , c , R_T , θ , p' , and D are, respectively, the virtual reflection height of the vertical signal, its correction for the curvature of the Earth, the Earth radius, the angle at the center of the Earth, the group path of the oblique signal, and the ground range associated to the oblique radio link. Combining the equations from (3) to (6), we obtain the conversion of the considered oblique ionogram into a vertical ionogram. This is done starting from the oblique ionogram in which for a frequency f_o can be deduced $p(f_o)$. From $p(f_o)$ ϕ is obtained through (6), where D is known. The ϕ is introduced in (4) to derive $h'(f_v)$. Finally, f_v is determined by (3).

4. Definition of the Quality Factor Q for the Improvement of the OIASA Performance

Besides the automatic interpretation of oblique ionograms, a further important issue of an autoscaling algorithm is being able to discard ionograms that even an expert operator could not interpret. This critical issue is also taken into account by the OIASA autoscaling algorithm. The contrast method used by OIASA to recognize the ordinary and extraordinary traces of ionospheric oblique soundings has proved to be also

(with $i = 1, \dots, m$ and $j = 1, \dots, n$) of the matrix A is an integer ranging from 0 to 255; proportional to the amplitude of received echo, this value is obtained directly from the data file recorded by the instrument.

To reduce the radio frequency (RF) noise without affecting important ionogram features, an additional simple original algorithm has been developed to filter the background noise from the image. An example of the results obtained can be seen in Figures 1a and 1b, in which is shown the same ionogram before and after applying such a filter algorithm. The filter algorithm analyzes each element a_{ij} of the matrix A and, when recognized as a component of the noise, it is eliminated. Since image background noise is often presented as dense sets of pixels, a defined number

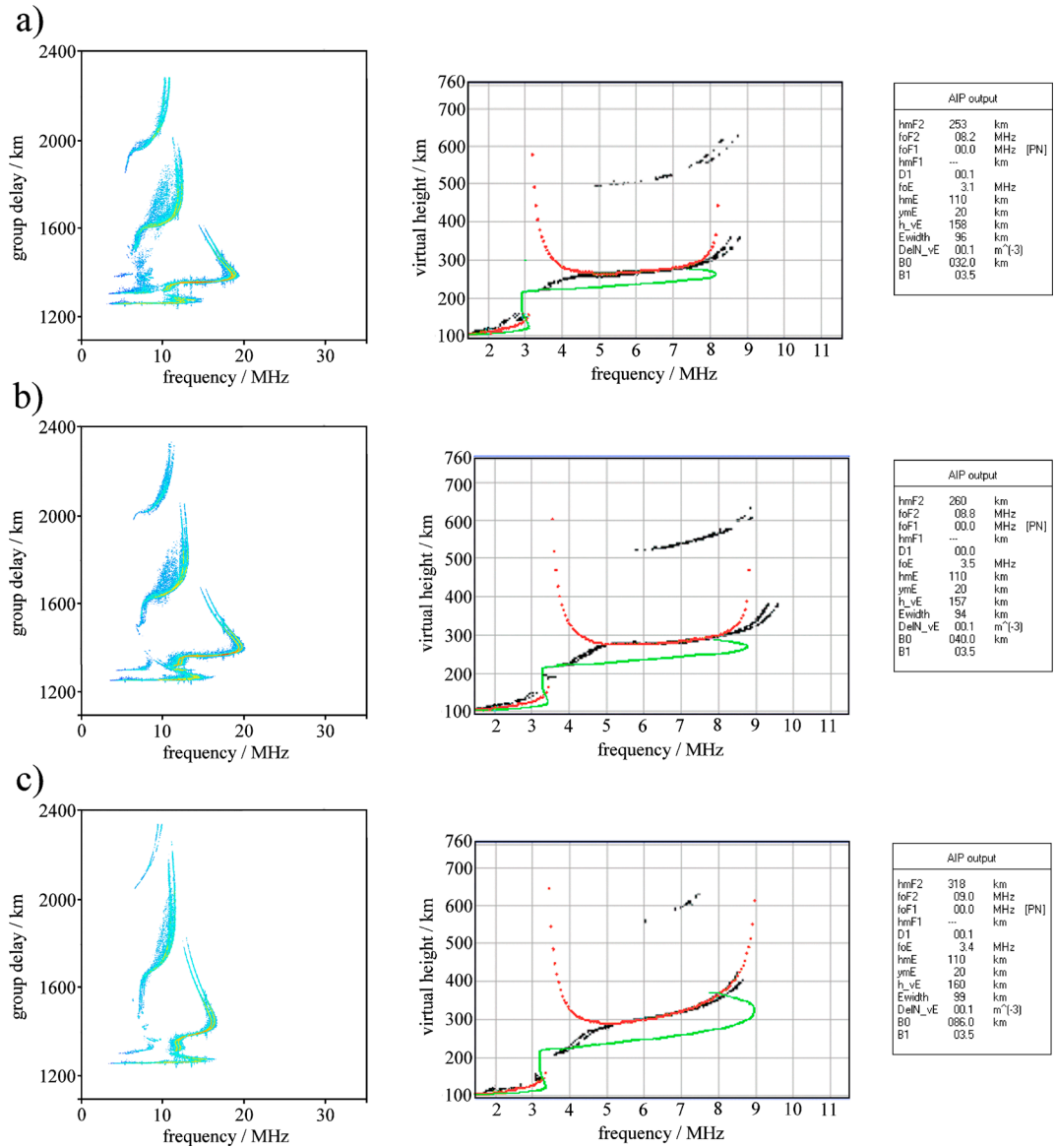


Figure 3. (a, b, and c) Examples of oblique ionograms converted into verticals. The results of the application of Autoscala program and the Adaptive Ionospheric Profiler (AIP) are also reported.

a useful method for discarding ionograms lacking data or those that are excessively noisy [Ippolito *et al.*, 2015]. In this method two empirical curves T_{ord} and T_{ext} which are able to fit the typical shape of the F_2 trace on the oblique ionograms, are defined for the detection of the ordinary and extraordinary traces, respectively. The local contrast C between T_{ord} and T_{ext} and A is then calculated making allowance for both the number of matched points and their amplitude. The curves T_{ord} and T_{ext} having the maximum value of C are then selected. If this value of C is greater than a fixed threshold C_t , the selected curves are considered as representative of the traces due to reflection from the F_2 region. Otherwise, no MUF value is provided as output, and the ionogram is deemed to lack sufficient information and is discarded. In this work we define a quality factor for the MUF values provided by OIASA, which will improve the reliability of the automatic scaling. The assessment of the false detections and the percentage of ionograms discarded is one of the main goals of this work: the results obtained will be discussed in the following and summarized in the conclusions. The equivalent vertical ionogram, resulting from the conversion of the original oblique ionogram, is stored in an RDF (Raw Data Format) file format and analyzed by Autoscala. This operation enables deriving all the ionospheric parameters over the midpoint of the oblique ray path, as shown in the examples in Figures 3a–3c. Autoscala

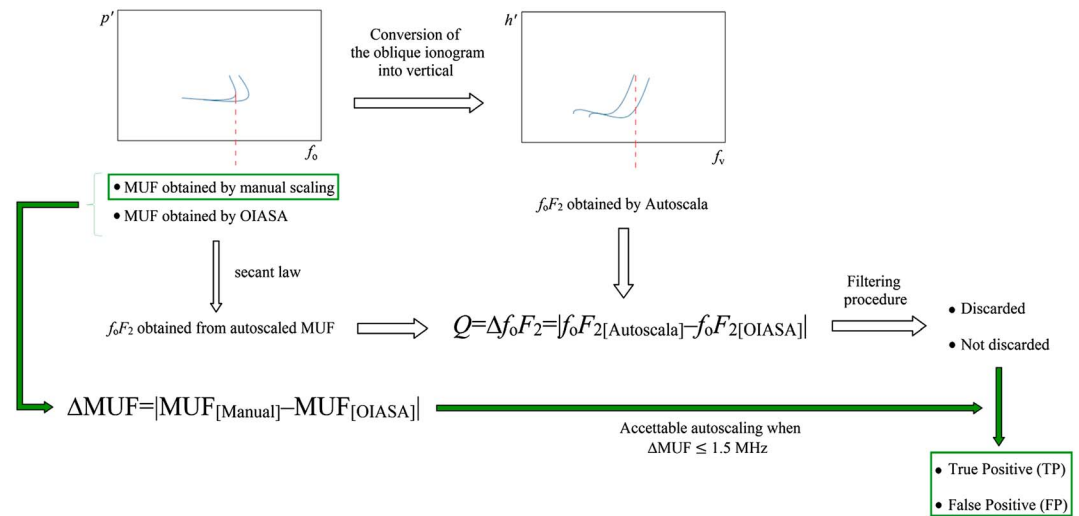


Figure 4. The system flow diagram of the whole algorithm, in which the quality factor Q is defined and used in a filtering procedure in order to decrease the false positive event percentage. Operations belonging to the procedure used to set the threshold value Q_t are marked by green arrows and boxes.

uses empirical curves to fit the typical shape of the F_2 , F_1 , and E_s [Scotto and Pezzopane, 2002a, 2002b; Pezzopane and Scotto, 2007, 2008; Scotto and Pezzopane, 2007] trace. Once different parts of the ionogram trace have been automatically identified, the electron density profile is estimated by an iterative technique to best fit a 12 free-parameter electron density profile model, called Adaptive Ionospheric Profiler (AIP), with the recorded ionogram [Scotto, 2009]. The critical frequency f_oF_2 given by Autoscala ($f_oF_{2[Autoscala]}$) is compared with $f_oF_{2[OIASA]}$, derived by the application of the secant law to the OIASA autoscaled MUF ($MUF_{[OIASA]}$):

$$f_oF_{2[OIASA]} = \frac{MUF_{[OIASA]}}{\sec \phi} \tag{7}$$

The parameter $Q = \Delta f_oF_2 = |f_oF_{2[Autoscala]} - f_oF_{2[OIASA]}|$ can be used, as shown in the next section, as a quality factor for the MUF values provided by OIASA. This can considerably decrease the false positive event occurrence, namely, the percentage of those ionograms for which the absolute value of the difference between the MUF obtained by OIASA and by a manual scaling procedure exceeds 1.5 MHz. The proposed procedure is schematically shown in Figure 4. An electron density profile $Ne(h)$ at the midpoint of the considered radio link is also estimated through the described technique, using the Adaptive Ionospheric Profiler (AIP), [Scotto, 2009].

The performance of the procedure presented in this paper was tested using a set of 384 high-quality ionograms, not previously filtered, from the Australian Bureau of Meteorology's Space Weather Services (SWS) campaign of oblique soundings, performed on the 1218 km path between the ionosondes of CUR, Australia (17.60°S; 123.82°E) and MTE, Australia (23.52°S; 133.68°E). The SWS oblique ionograms were recorded using a Digital Oblique Receiving System (DORS) on loan from the Australian Defence Science and Technology group (DST). As reported in Tables 1a and 1b, for all the ionograms of the data set, an experienced operator has been able to scale a MUF value which has been assumed as reference. We define as

Table 1a. The Behavior of OIASA to Reject Ionograms With Insufficient Information Without Using Any Filtering Procedure^a

	Scaled by the Software		Discarded by the Software	
	No. of Cases	(%)	No. of Cases	(%)
The operator did not scale the MUF	0	0	0	0
The operator scaled the MUF	384	100	0	0
Total	384		0	

^aThe analyzed data set is made by 384 high-quality oblique ionograms taken by SWS.

Table 1b. Accurate and Acceptable Values for OIASA Application on the Same Ionograms Data Set [Ippolito et al., 2015]^a
Scaled by the Software and the Operator

	No. of Cases	(%)
Accurate	345	89.84
Acceptable	373	97.14
Total	384	

^aThe automatic scaling algorithm has been improved and a percentage of 97.14% of ionograms with acceptable MUF values has been achieved, increasing of 1.04% the result obtained by Ippolito et al. [2015].

“Accurate” MUF values in the range of 0.5 MHz from the manual scaled MUF, while values in the range of 1.5 MHz are defined as “Acceptable,” in accordance with the International Union of Radio Science (URSI) standard [Piggott and Rawer, 1972]. The filtering procedure, which defines a quality factor for the MUF values provided by the autoscaling algorithm, has been applied to the 384 oblique ionograms of the analyzed data set. For each ionogram, the corresponding values of f_oF_2 [Autoscala] and f_oF_2 [OIASA] have been identified. Autoscala did not provide an f_oF_2 value for 18 equivalent vertical ionograms; consequently, no value of Q has been associated to them. For these ionograms was not possible to apply the automatic rejection procedure, based on Q . Different Q_t values have been tested, using the receiver operating characteristic (ROC) curve method, in order to evaluate the appropriate threshold Q_t . Once the Q value is selected, all the procedure is automated. In Figure 5 we show, by varying the Q_t threshold, the graphical plot of the true positive rate (TPR) versus false positive rate (FPR), for the binary classifier system described in this work. For each tested value of Q_t , a fraction of autoscaled oblique ionograms is correctly classified as positive by the filter and represents the TP (true positive), while the remaining fraction FP (false positive) is incorrectly classified as positive by the filtering procedure. The closer the ROC curve approaches the upper left corner of the plot, the higher the overall accuracy of the test [Brown and Davis, 2006]. Following this approach the Q_t threshold value has been set to 1.7 MHz. In Table 2 we present the comparison between the behavior of the OIASA autoscaling algorithm without using the filtering procedure and applying it with a Q_t value set to 1.7 MHz. In case of applying the filter, it can be seen that a further number of ionograms for which the difference between manually scaled MUF and autoscaled MUF was greater than 1.5 MHz have been successfully discarded. As a consequence, the true positive events percentage is not altered, while the false positive events percentage decreases from 2.86% to 1.82%.

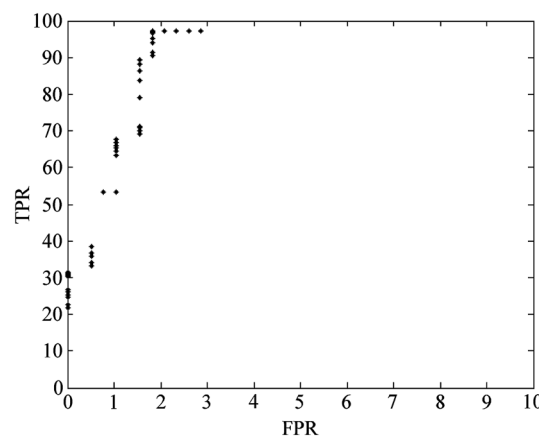


Figure 5. The ROC curve for the binary classifier described in this work, where TPR (true positive rate) and FPR (false positive rate) are TP (true positive) and FP (false positive) fractions expressed as percentages. As the quality of the oblique ionograms is high, the FPR values are always less than 3%. According to this curve the Q_t value was set to 1.7 MHz, since it represents the best result achieved as the value approaches the top left of the plot.

5. Conclusions

A quality factor Q to improve the rejection capabilities of OIASA program has been defined in this work. A set of 384 high-quality oblique soundings have been inverted into vertical ionograms and then analyzed by the Autoscala program. We have defined Q as the difference between the critical frequency f_oF_2 value given by Autoscala f_oF_2 [Autoscala] and f_oF_2 [OIASA] which represents the critical frequency obtained from the MUF autoscaled by OIASA through the secant law. For different values of Q the difference between the manually scaled MUF and the autoscaled MUF was calculated. Applying the Q as a filter for the oblique ionograms to be scaled by OIASA, further oblique ionograms that lacked information on the state of the ionosphere were discarded. Through the ROC curve method, we have identified a threshold value Q_t which provides the best performance of the filter. Without using the Q filter, 373 of the 384 oblique ionograms, the OIASA algorithm provides a MUF

Table 2. Comparison Between the Behavior of OIASA Without Applying the Filtering Procedure and Applying the Filtering Procedure^a

	Results Without Q Filter		Results With Q Filter	
	No. of Cases	(%)	No. of Cases	(%)
Well scaled ($\Delta\text{MUF} < 1.5$ MHz)	373	97.14	373	97.14
Bad scaled ($\Delta\text{MUF} > 1.5$ MHz)	11	2.86	7	1.82
Discarded	0	0	4	1.04
Total	384		384	

^aThe Q_f value of the filter is set to 1.7 MHz. A data set of 384 high-quality oblique ionograms has been considered. It can be notice how the true positive events percentage is not altered, while the false positive events percentage decreases from 2.86% to 1.82% .

value within the range of 1.5 MHz from the manual scaled MUF, while no ionograms were automatically discarded. This resulted in 11 out of the 384 oblique ionograms deemed as being false positive events at a rate of 2.86%. When applying the Q filter, it was found that 373 of the 384 oblique ionograms had been scaled correctly by the OIASA software ($\Delta\text{MUF} < 1.5$ MHz), 4 ionograms were automatically discarded and 7 were deemed to have been incorrectly scaled by the software ($\Delta\text{MUF} > 1.5$ MHz). In this case the false positive event percentage decreases from 2.86% to 1.82%. The algorithm described in this work is an efficient method to improve the performance of OIASA, which can be proposed as a system to obtain the real-time MUF from oblique ionograms.

References

- Bibl, K. (1998), Evolution of the ionosonde, *Ann. Geofis.*, *41*, 667–680.
- Brown, C. D., and H. T. Davis (2006), Receiver operating characteristics curves and related decision measures: A tutorial, *Chemom. Intell. Lab. Syst.*, *80*, 24–38.
- Cushley, A. C., and J.-M. Noel (2014), Ionospheric tomography using ADS-B signals, *Radio Sci.*, *49*, 549–563, doi:10.1002/2013RS005354.
- Galkin, I. A., G. M. Khmyrov, A. V. Kozlov, B. W. Reinisch, X. Huang, and V. V. Paznukhov (2008), The ARTIST 5, in *Radio Sounding and Plasma Physics*, AIP Conference Proceedings, vol. 974, pp. 150–159, doi:10.1063/1.2885024.
- Galkin, I. A., B. W. Reinisch, X. Huang, and D. Bilitza (2012), Assimilation of GIRO data into a real-time IRI, *Radio Sci.*, *47*, RS0L07, doi:10.1029/2011RS004952.
- Gething, P. J. D. (1969), The calculation of electron density profiles from oblique ionograms, *J. Atmos. Terr. Phys.*, *31*, 347–354.
- Gething, P. J. D., and R. G. Maliphant (1967), Unz's application of Schlomilch's integral equation to oblique incidence observations, *J. Atmos. Terr. Phys.*, *29*, 599–600.
- Gilbert, J. D., and R. W. Smith (1988), A comparison between the automatic ionogram scaling system ARTIST and the standard manual method, *Radio Sci.*, *23*(6), 968–974, doi:10.1029/RS023i006p00968.
- Heaviside, O. (1902), *Telegraphy*, Encyclopaedia Britannica, Edimburgh.
- Ippolito, A., C. Scotto, M. Francis, A. Settini, and C. Cesaroni (2015), Automatic interpretation of oblique ionograms, *Adv. Space Res.*, *55*, 1624–1629.
- Jin, S. G., J. U. Park, J. L. Wang, B. K. Choi, and P. H. Park (2006), Electron density profiles derived from ground-based GPS observations, *J. Navig.*, *59*(3), 395–401, doi:10.1017/S0373463306003821.
- Kennelly, A. E. (1902), Research in telegraphy, *Elec. World Eng.*, *6*, 473.
- Kol'tsov, V. V. (1969), Determination of virtual reflection heights from oblique sounding data, *Geomagn. Aeron. (USSR)*, *9*(5), 698–701.
- Lodge, O. (1902), Mr Marconi's results in day and night wireless telegraphy, *Nature*, *66*, 222.
- Martyn, D. F. (1935), The propagation of medium radio waves in the ionosphere, *Proc. Phys. Soc.*, *47*, 323–339.
- Pezzopane, M., and C. Scotto (2007), The Automatic Scaling of Critical Frequency f_oF_2 and MUF(3000)F2: a comparison between Autoscala and ARTIST 4.5 on Rome data, *Radio Sci.*, *42*, RS4003, doi:10.1029/2006RS003581.
- Pezzopane, M., and C. Scotto (2008), A method for automatic scaling of F_1 critical frequency from ionograms, *Radio Sci.*, *43*, RS2591, doi:10.1029/2007RS003723.
- Phanivong, B., J. Chen, P. L. Dyson, and J. A. Bennet (1995), Inversion of oblique ionograms including the Earth's magnetic field, *J. Atmos. Terr. Phys.*, *57*, 1715–1721.
- Piggott, W. R., and K. Rawer (1972), *U.R.S.I. Handbook of Ionogram Interpretation and Reduction*, US Department of Commerce National Oceanic and Atmospheric Administration-Environmental Data Service, Asheville, N. C.
- Redding, N. J. (1996), The autoscaling of oblique ionograms, Research report DSTO-RR-0074.
- Reilly, M. H., and J. D. Kolesar (1989), A method for real height analysis of oblique ionograms, *Radio Sci.*, *24*, 575–583, doi:10.1029/RS024i004p00575.
- Reinisch, B. W., and X. Huang (1983), Automatic calculation of electron density profiles from digital ionograms: 3. Processing of bottomside ionograms, *Radio Sci.*, *18*(3), 477–492, doi:10.1029/RS018i003p00477.
- Scotto, C. (2009), Electron density profile calculation technique for Autoscala ionogram analysis, *Adv. Space Res.*, *44*(6), 756–766, doi:10.1016/j.asr.2009.04.037.
- Scotto, C., and M. Pezzopane (2002a), A software for automatic scaling of f_oF_2 and MUF(3000)F2 from ionograms, in *Proceedings of URSI 2002*, Maastricht, 17–24 August, 2002 (on CD).
- Scotto, C., and M. Pezzopane (2002b), A software for automatic scaling of f_oF_2 and MUF(3000)F2 from ionograms, URSI XXVII General Assembly. [Available at <http://www.ursi.org/Proceedings/ProcGA02/papers/p1018.pdf>.]
- Scotto, C., and M. Pezzopane (2007), A method for automatic scaling of sporadic E layers from ionograms, *Radio Sci.*, *42*, RS2012, doi:10.1029/2006RS003461.
- Scotto, C., and M. Pezzopane (2008), Removing multiple reflections from the F_2 layer to improve Autoscala performance, *J. Atmos. Sol. Terr. Phys.*, *70*, 1929–1934.